






The molecular landscape and associated clinical experience in infant medulloblastoma: prognostic significance of second-generation subtypes

D. Hicks*, G. Rafiee*[†], E. C. Schwalbe*[‡], C. I. Howell*, J. C. Lindsey*, R. M. Hill*, A. J. Smith*, P. Adidharma*, C. Steel*, S. Richardson*, L. Pease*, M. Danilenko*, S. Crosier*, A. Joshi[§], S. B. Wharton[¶] , T. S. Jacques** , B. Pizer^{††}, A. Michalski**, D. Williamson*, S. Bailey* and S. C. Clifford* 

*Wolfson Childhood Cancer Research Centre, Newcastle University Centre for Cancer, Translational and Clinical Research Institute, Newcastle University, Newcastle upon Tyne, [†]School of Electronics, Electrical Engineering and Computer Science, Queen's University Belfast, Belfast, [‡]Department of Applied Sciences, Northumbria University, Newcastle upon Tyne, [§]Department of Neuropathology, Royal Victoria Infirmary, Newcastle University Teaching Hospitals NHS Foundation Trust, Newcastle upon Tyne, [¶]Sheffield Institute for Translational Neuroscience, University of Sheffield, Sheffield, **Great Ormond Street Hospital, London and ^{††}Institute of Translational Research, University of Liverpool, Liverpool, UK

D. Hicks, G. Rafiee, E. C. Schwalbe, C. I. Howell, J. C. Lindsey, R. M. Hill, A. Smith, P. Adidharma, C. Steel, S. Richardson, L. Pease, M. Danilenko, S. Crosier, A. Joshi, S. Wharton, T. Jacques, B. Pizer, A. Michalski, D. Williamson, S. Bailey and S. C. Clifford (2020) *Neuropathology and Applied Neurobiology*

The molecular landscape and associated clinical experience in infant medulloblastoma: prognostic significance of second-generation subtypes

Aims: Biomarker-driven therapies have not been developed for infant medulloblastoma (iMB). We sought to robustly sub-classify iMB, and proffer strategies for personalized, risk-adapted therapies. **Methods:** We characterized the iMB molecular landscape, including second-generation subtyping, and the associated retrospective clinical experience, using large independent discovery/validation cohorts (n = 387). **Results:** iMB_{Grp3} (42%) and iMB_{SHH} (40%) subgroups predominated. iMB_{Grp3} harboured second-generation subtypes II/III/IV. Subtype II strongly associated with large-cell/anaplastic pathology (LCA; 23%) and *MYC* amplification (19%), defining a very-high-risk group (0% 10yr overall survival (OS)), which progressed rapidly on all therapies; novel approaches are urgently required. Subtype VII (predominant within iMB_{Grp4}) and subtype IV tumours were standard risk (80% OS) using upfront CSI-based therapies; randomized-controlled trials of upfront

radiation-sparing and/or second-line radiotherapy should be considered. Seventy-five per cent of iMB_{SHH} showed DN/MBEN histopathology in discovery and validation cohorts ($P < 0.0001$); central pathology review determined diagnosis of histological variants to WHO standards. In multivariable models, non-DN/MBEN pathology was associated significantly with worse outcomes within iMB_{SHH}. iMB_{SHH} harboured two distinct subtypes (iMB_{SHH-I/II}). Within the discriminated favourable-risk iMB_{SHH} DN/MBEN patient group, iMB_{SHH-II} had significantly better progression-free survival than iMB_{SHH-I}, offering opportunities for risk-adapted stratification of upfront therapies. Both iMB_{SHH-I} and iMB_{SHH-II} showed notable rescue rates (56% combined post-relapse survival), further supporting delay of irradiation. Survival models and risk factors described were reproducible in independent cohorts, strongly supporting their further investigation and development.

Correspondence: Steven C. Clifford, Wolfson Childhood Cancer Research Centre, Newcastle University Centre for Cancer, Translational and Clinical Research Institute, Newcastle University, Newcastle upon Tyne, NE1 7RU, UK. Tel: +44 (0)191 208 2239. Fax: +44 (0) 191 208 4301. E-mail: steve.clifford@ncl.ac.uk

© 2020 The Authors. *Neuropathology and Applied Neurobiology* published by John Wiley & Sons Ltd on behalf of British Neuropathological Society.

This is an open access article under the terms of the Creative Commons Attribution License, which permits use, distribution and reproduction in any medium, provided the original work is properly cited.

Conclusions: Investigations of large, retrospective cohorts have enabled the comprehensive and robust characterization of molecular heterogeneity within iMB.

Novel subtypes are clinically significant and subgroup-dependent survival models highlight opportunities for biomarker-directed therapies.

Keywords: Infant medulloblastoma, paediatric oncology, molecular pathology, risk stratification, biomarkers

Introduction

Medulloblastoma (MB), the most common malignant paediatric brain tumour, accounts for around 10% of childhood cancer deaths. Five-year overall survival (OS) rates of approximately 70% are currently achieved in non-infants (children aged over either 3 or 5 years at diagnosis, depending on national treatment philosophies) using contemporary multimodal therapies (maximal surgical resection, cranio-spinal irradiation (CSI) and adjuvant combination chemotherapy)[1].

Infant medulloblastomas (iMB; ~30% of all MB patients) are associated with a poorer prognosis (5-year OS <60%) and are treated using separate approaches. Current iMB protocols aim to minimize the permanently disabling late effects associated with irradiation of the developing brain by avoidance/delay of CSI [2]. However, this must be balanced with morbidity and mortality, and any potential for salvage using CSI at a later stage [3]. Desmoplastic nodular/medulloblastoma with extensive nodularity (DN/MBEN) pathology [4] (~40% of iMB; favourable risk) is the only clinically adopted prognostic risk factor and is used as a basis for de-escalation of treatment [5]; no molecular biomarkers are in current clinical use.

Recent years have seen significant advances in our understanding of the disease-wide molecular pathology of medulloblastoma. The 2016 World Health Organisation (WHO) classification of brain tumours recognizes four consensus molecular subgroups (MB_{WNT} , MB_{SHH} , MB_{Grp3} , and MB_{Grp4}) [4], however, recent studies, enabled by increased cohort sizes and profiling resolution, have identified intra-subgroup heterogeneity and described further molecular subtypes within these subgroups [6-10]. Importantly, subgroup-directed targeted and risk-adapted therapies are now in clinical trials for non-infant medulloblastoma based on evidence from biological studies in large retrospective cohorts and clinical trials [11-13]. An equivalent evidence base does not exist for iMB, which has, to date, typically

only been considered biologically as part of disease-wide studies.

The first dedicated studies of the genomic landscape of iMB are only now emerging, including first prospective characterization of clinical trials cohorts [7,14,15]. Initial findings with clinical potential have emerged. iMB_{SHH} subtypes have been described, however, studies of their clinical significance have been based on modestly-sized clinical cohorts ($n = 25$ [14], $n = 76$ [7] and $n = 28$ [15]) and findings are inconsistent, potentially due to cohort and treatment differences, and limited statistical power, within these cohorts. These observations now require further investigation. Importantly, these studies have focused on specific subgroups (i.e. DN/MBEN MB_{SHH} [7], non-metastatic DN/MBEN MB_{SHH} [15]) and have not explored biological and clinical heterogeneity within the majority of iMB (non-DN/MBEN and non-SHH tumours represent ~60-70% of all iMBs).

Critically, large-scale, systematic biological studies are urgently required to establish the molecular landscape across all iMB disease – including incidence, biological and clinical relevance of molecular features and novel subtypes (e.g. Group3/4 subtypes, iMB_{SHH} subtypes [10,13,15]) – to support future clinical advances. In view of the limited clinical studies with biological annotation which have been undertaken to date, the collection and characterization of retrospective iMB cohorts offers the prime current opportunity to address these challenges. Importantly, in view of current strategies towards treatment of iMB with radiation-sparing approaches [15,16], and the common historical use of radiotherapy, its impact must be carefully considered in such retrospective studies.

We report comprehensive characterization of the molecular pathology of iMB using large historical cohorts, encompassing discovery in 202 patients with full centrally reviewed clinical and pathological annotation, and validation in 185 independent patients. We demonstrate that iMBs harbour distinct biological

characteristics and clinically significant molecular subtypes within the core molecular subgroups. Using these factors, reproducible molecular subgroup-directed disease sub-classification and risk-stratification models could be derived which are independent of upfront radiotherapy and outperform current clinico-pathological schemes. These models provide a basis for personalized therapies, improved therapeutic strategies and future clinical trials.

Materials and Methods

Study cohorts

A primary discovery cohort of 202 infant tumours, <5.0 years of age (median 2.61 years) on the date of first-line surgery, was assembled from UK Children's Cancer and Leukaemia Group (CCLG) institutions and collaborating centres. All patients had systematic central clinical review and follow up ≥ 5 years. Central review of histological variants was performed to WHO 2016 criteria [4]. Full demographic and clinical data, including treatment protocols, are given in the Tables S1-S2. Importantly, considering the retrospective nature of the cohort, survival and sub-total resection (STR) rates were equivalent across the ascertainment period (data not shown), and patients collected post-1990 received radiotherapy at equivalent rates. A non-infant comparator cohort (patients ages 5–16 years at diagnosis) is detailed in Table S3. Additional independent iMB cohorts [6,8] were used for the discovery and validation of clinical and molecular features and for these, institutional annotation was used. Full details of external cohorts and subsets used thereof are given in Table S3, including cohort selection criteria.

Procedures

Tumours were assigned to the four consensus medulloblastoma molecular subgroups (MB_{WNT} , MB_{SHH} , MB_{Grp3} and MB_{Grp4}) using established DNA methylation array-based methods [17]. Chromosome arm-level copy number aberrations (CNAs) were derived from these data as previously described [18]. *TP53* status was assessed in iMB_{SHH} where possible [4]. To identify heterogeneity within iMB_{SHH} , class discovery was first undertaken using methylation array data for our primary discovery tumour cohort, then applied to two

published datasets [6, 8], together totalling 147 iMB_{SHH} patients (see Data S1). Tumours were assigned to subgroups using a consensus of non-negative matrix factorization (NMF) [9] and t-SNE/dbSCAN [8] clustering, as previously described. For iMB_{Grp3} , second-generation subtypes were assigned to the combined primary discovery and validation cohorts (detailed in the Data S1) according to the 'Grp3 and Grp4 Classifier' found at <https://www.moleculareuropathology.org/mnp/classifier/7>; Accession numbers for DNA methylation array profiles used for the determination of molecular subgroup/subtype status are GSE93646 [9], GSE85218 [8] (Gene Expression Omnibus) and EGAS00001001953 [6] (European Genome-Phenome Archive).

Copy number status of *MYC* and *MYCN* was defined by consensus of ≥ 2 of the following methods; iFISH [19,20], MLPA, Affymetrix Genome-Wide Human SNP Array 6.0 and/or Illumina HumanMethylation450 DNA methylation array [18]. Mutational data for *KMT2D*, *SUFU*, *PTCH1* and *TP53* in our primary discovery cohort were generated using the SureSelect target capture system (Agilent) and subsequent sequencing on the Illumina HiSeq2500 instrument.

Statistical and survival analyses

All clinico-molecular features assessed in the study are listed in Table S4; associations between features were assessed by Chi-squared and Fisher's exact tests. Univariable and multivariable Cox proportional hazards tests were used to investigate the association of features with survival. Analysis was performed using SPSS v23 (SPSS, Chicago, U.S.A.) and the R statistical environment (version 3.2.3).

Expanded methodological and statistical detail can be found in the Data S1.

Results

Key medulloblastoma features were differentially distributed between iMB (<5.0 years, $n = 202$) and non-infants (5-16 years, $n = 262$) (Figure 1a, Figure S1). As expected, iMB_{SHH} (63/163, 39%) and iMB_{Grp3} (69/163, 42%) were the predominant molecular subgroups and displayed distinct molecular pathologies; iMB_{Grp4} was less common ($n = 29/163$, 18%) and WNT tumours were largely absent (2 patients; 4.7 and 4.9 years old at diagnosis) (Table S5, Figures S1-S2).

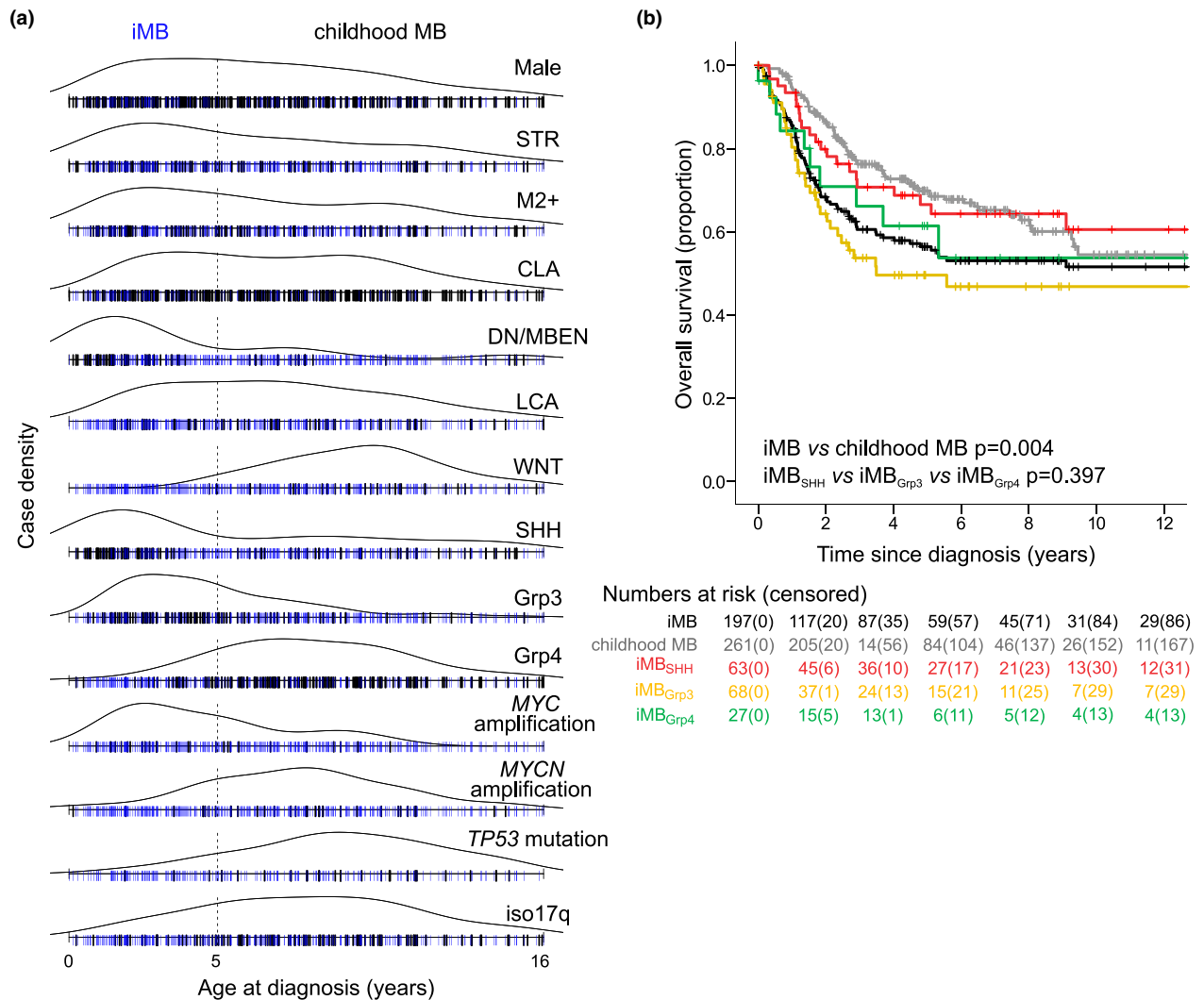


Figure 1. Biological and clinical features of iMB differ significantly from the non-infant disease. (a) Incidence of demographic, clinical, pathological and biological features across the age range 0-16 years, dotted line represents 5-year age at diagnosis threshold for infant definition in this study. Abbreviations used CLA, classic; DN/MBEN, desmoplastic/nodular, medulloblastoma with extensive nodularity; LCA, large-cell/anaplastic; iso17q, isochromosome 17q. (b) Overall survival (OS) Kaplan-Meier plot of children (childhood MB, grey curve), all infants (iMB, black curve) and all infants by molecular subgroup (iMB_{SHH}, red curve; iMB_{Grp3}, yellow curve; iMB_{Grp4}, green curve), with at risk table (number censored in parentheses). P values are from log-rank test

Within iMB, survival was equivalent between consensus molecular subgroups (5yr OS; iMB_{SHH} 66% vs. iMB_{Grp3} 50% vs. iMB_{Grp4} 61%, log rank $P = 0.397$) (5yr PFS; iMB_{SHH} 53% vs. iMB_{Grp3} 50% vs. iMB_{Grp4} 65%) (Figure 1b, Table S5). We thus sought to explore the potential of further molecular heterogeneity, including novel subtypes, to account for survival differences within these groups. Fifty-eight per cent of our cohort received upfront cranio-spinal radiation; we therefore

sought to understand its interaction with prognostic features.

Within iMB_{SHH}, two robust subgroups were identified in our primary discovery cohort (Figure 2a, Figure S3a-c) using non-negative matrix factorization (NMF) and t-SNE/dbSCAN. These were recapitulated when derived in a larger, combined, cohort that included external cohorts [6,8] not previously used for iMB-specific assessment (Figure S3d-g). iMB_{SHH-I} was

highly associated with the recently reported SHH- β group, whereas iMB_{SHH-II} was enriched for SHH- α and - γ ($P < 0.0001$, Figure S3h) [8]. In view of this, subgroup reproducibility/validation within our study and compatibility of clinico-molecular correlates across studies [7,15], the naming convention of iMB_{SHH-I} and iMB_{SHH-II} was followed for clarity.

iMB_{SHH} overall presented at a younger age (vs. iMB_{Grp3}; median age 1.9 years vs. 2.8 years at diagnosis ($P < 0.0001$), however, iMB_{SHH-I} tumours presented later than iMB_{SHH-II} (median age 2.0 years vs. 1.4 years, $P = 0.026$; Figure S3i). Overall, iMB_{SHH} was strongly but not exclusively associated with DN/MBEN pathologies (45/63, 71%) (Figure 2b, $P < 0.0001$, Figure S4); three DN/MBEN tumours in our cohort were iMB_{Grp4}. However, notable frequencies of CLA ($n = 10$, 17%) and LCA ($n = 4$, 7%) tumours were also observed within iMB_{SHH} (Figure 2c). Patients with these non-DN/MBEN MB_{SHH} tumours presented at an older age ($P = 0.047$, Figure 2d). Mutations in *PTCH1* and *SUFU* were exclusively associated with iMB_{SHH} (*PTCH1*, 12/26, 46%, $P = 0.002$; *SUFU*, 7/26, 27%, $P = 0.0071$) but were equivalently distributed between iMB_{SHH-I} and iMB_{SHH-II}. Within iMB_{SHH}, iMB_{SHH-I} was significantly enriched for classic pathology ($P = 0.04$), *KMT2D* mutations ($P = 0.001$, exclusive to iMB_{SHH-I}), chromosome 2 gain ($P = 0.009$) and loss of 20p ($P = 0.016$) (Figure 2a). iMB_{SHH-II} had a significant enrichment of MBEN pathology ($P = 0.049$), 9p gain ($P = 0.012$) and losses of 10q ($P = 0.016$) and 9q ($P < 0.001$). Where assessable, these associations validated in independent cohorts (Figure S2).

iMB_{SHH} patients within our cohort were treated heterogeneously, both at diagnosis and relapse (Table S1). We therefore first assessed whether consistent predictors of overall survival were observed across iMB_{SHH} cohorts. STR (HR 6.7, CI 2.5-17.6, $P < 0.001$) and chromosome 9p gain (HR 3.3, CI 1.1-9.7, $P = 0.026$) were significantly associated with poorer OS, while DN/MBEN pathology (HR 0.2, CI 0.1-0.5, $P = 0.001$) conferred a favourable risk (Figure 2e). No other features tested (Table S4), including the novel intra-iMB_{SHH} molecular subtypes, metastatic disease status or treatment variables, were significantly associated with OS. OS was equivalent between DN and MBEN pathological variants (Figure S5e).

Based on these findings, iMB_{SHH} was considered as a single subgroup in cross-validated multivariable Cox

modelling of OS; this identified STR (HR 6.4 CI 2.2-17.8, $P < 0.0001$) and DN/MBEN pathology (HR 0.5, CI 0.3-0.8, $P = 0.004$) as independent prognostic risk factors (Figure 2e), which validated in an independent cohort [8] (Figure S6b). CLA/LCA and/or STR iMB_{SHH} tumours represented a very high-risk group (VHR; 5yr OS 26%), with >5-fold relative-risk (log rank $P < 0.0001$) compared to totally resected DN/MBEN favourable-risk disease (FR; 5yr OS 93%) (Figure 2f-g). These relationships were observed consistently, independent of whether upfront radiotherapy was received (Figure S5c).

We next assessed novel second-generation molecular subtypes I-VIII [10] within iMB_{Grp3} and iMB_{Grp4}, and their clinico-molecular correlates, based on a combined analysis of our primary iMB_{Grp3} discovery cohort and iMB_{Grp3} tumours derived from two disease-wide external cohorts [6,8] (total $n = 146$, Table S3). In iMB_{Grp3}, subtypes II (29%), III (21%) and IV ($n = 44$) predominated. Subtype IV was significantly associated with an earlier age at diagnosis (<3ys, $P < 0.0001$), many frequent CNAs and better OS (80% 5yr OS) (Figure 3a-b). Subtype II was enriched for LCA pathology ($P < 0.001$), *MYC* amplification ($P < 0.0001$), i17q ($P = 0.001$) and gains of chromosome 1q, 5, 6 and 8 (all $P < 0.005$) and, expectedly given the enrichment of high-risk features, had a relatively poorer 5yr OS of 32%. Subtype III had significantly fewer CNAs than subtypes II and IV ($P < 0.001$) but no other characteristic features, with a 5yr OS of 38%. iMB_{Grp3} samples were occasionally, but rarely classified as subtypes V (5yr OS 63%), I (5yr OS 60%) and VII (5yr OS 80%); these subtypes were heavily enriched for iMB_{Grp4} samples; subtypes VI (5yr OS 80%) and VIII (5yr OS 83%) were exclusively iMB_{Grp4} (shown for reference; Figure 3a-b). These associations also validated in independent cohorts (Figure S2) [6,8]. Mutations were infrequent in all iMB_{Grp3} and iMB_{Grp4} subtypes.

Notably, iMB_{Grp3} patients in our cohort were commonly treated with upfront radiotherapy, which may contribute to survival rates observed for subtypes IV and VII (i.e. >75% OS, Figure 3). We therefore undertook univariable and multivariable analyses of overall survival within iMB_{Grp3}, considering all clinical, molecular and treatment factors. In univariable analyses, *MYC* amplification, LCA pathology, receipt of chemotherapy only, isochromosome 17q and subtype II were significantly associated with poorer OS

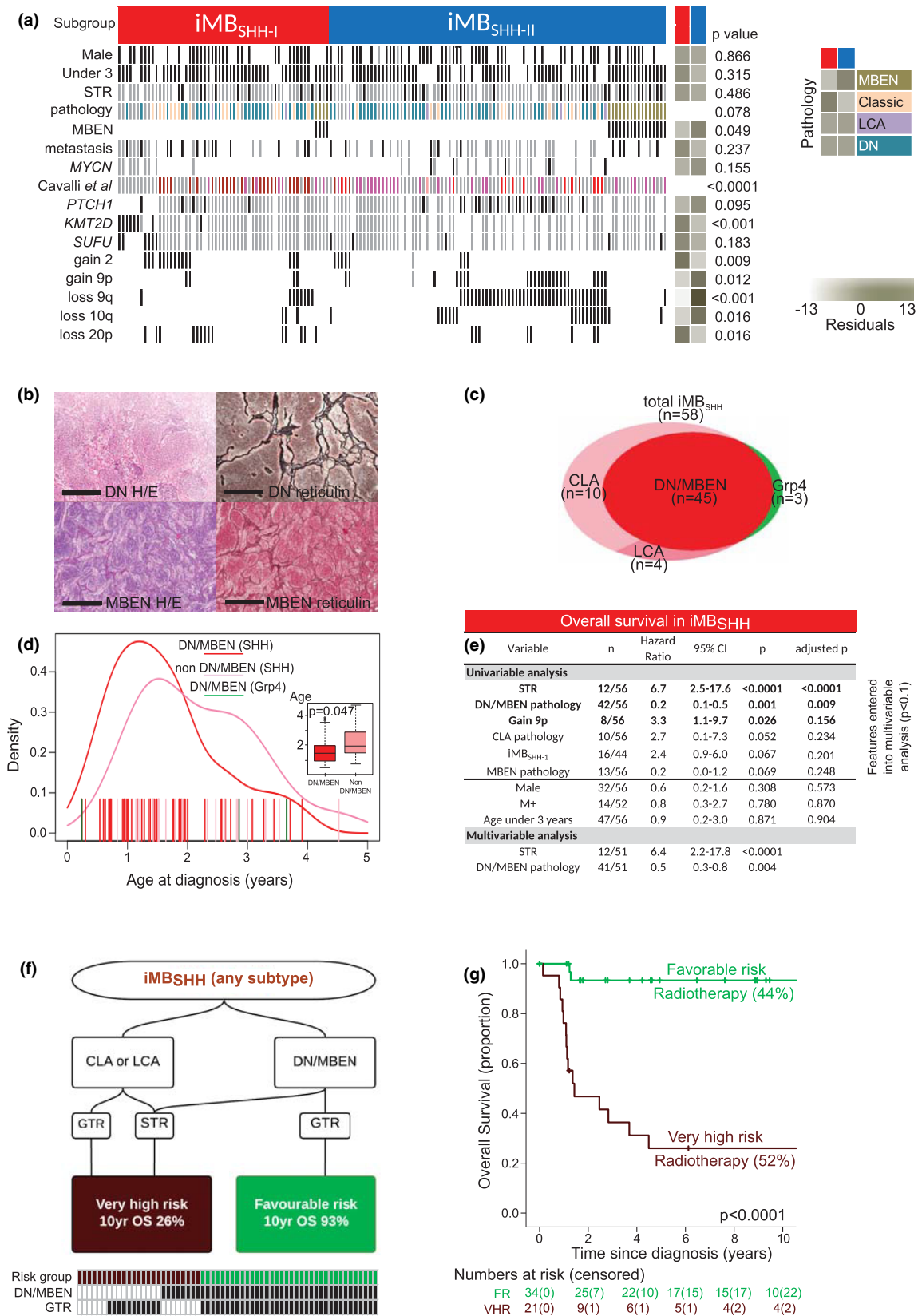


Figure 2. The molecular landscape of iMB_{SHH} and associated retrospective clinical experience. (a) Clinico-pathological and molecular disease features are differentially distributed in iMB_{SHH} subgroups. Membership is derived from unsupervised NMF clustering and tSNE/dbSCAN techniques in a combined methylation array dataset (n = 155). Residuals from Fisher's exact or χ^2 tests indicate where subgroup enrichment has occurred (darker shades indicate stronger relationships); scale bar for residuals is shown. Black bar, positive for feature; unfilled, negative for feature; grey bar, data unavailable. (b) Micrographs of H&E (haematoxylin and eosin; for general cell morphology) and reticulin (for collagen fibres) in DN (desmoplastic/nodular) and MBEN (medulloblastoma with extensive nodularity) tumours. Scale bar = 500 μ m. (c) Euler diagram showing overlap of pathology variant with iMB subgroup status. (d) Case density of age at diagnosis in iMB_{SHH} DN/MBEN (red line), iMB_{SHH} non-DN/MBEN (pink) and iMB_{Grp4} DN/MBEN (green) groups. Box and whiskers plot and statistical test is inset. (e) Univariable and multivariable Cox proportional hazards regression model of overall survival in discovery cohort iMB_{SHH}. Features which entered multivariable analysis ($P < 0.1$, above line; $P < 0.05$ shown in bold font) are indicated. Cox proportional hazards test is shown either uncorrected (p) or corrected for multiple testing by the Benjamini-Hochberg method (adjusted p). Additional clinical features are shown for reference (gender, age under 3 years, metastasis). (f) Summary of a novel risk-stratification scheme for overall survival in iMB_{SHH}. G. Kaplan-Meier plot of iMB_{SHH} risk stratification model. At risk table (number censored in parentheses) and log-rank test is shown. Abbreviations: STR, sub-total resection; CLA, classic; LCA, large cell/anaplastic; DN/MBEN, desmoplastic nodular/ medulloblastoma with extensive nodularity; SHH, sonic hedgehog; CI, confidence interval; FR, favourable risk; VHR, very high risk; M+, metastatic disease M2 or above

(Figure 3c). Conversely, subtype IV, receipt of radiotherapy and losses of chromosomes 10 and 11 predicted a better OS. Multivariable Cox modelling identified *MYC* amplification (HR 4.9, CI 2.0-12.0, $P < 0.001$) and LCA pathology (HR 2.4, CI 1.4-4.3, $P = 0.003$) as the only independently prognostic risk factors. Presence of either feature defined a very high-risk group (VHR; 27% (16/62); 5yr OS 0%), with typically very short median times to relapse (4 months) and death (5months); outcomes for this patient group were universally dismal – in both radiotherapy-treated and radio-naïve patients (Figure 3, Figure S7). Remaining CLA, non-*MYC* amplified iMB_{Grp3} tumours were high risk (HR; 73% (46/62); 10yr OS 73%) (Figure 3d-e); 36/46 (78%) of these patients were treated upfront with radiotherapy. These relationships validated in an independent cohort (Figure S6) [8]. Most patients who rapidly progressed on treatment belonged to the iMB_{Grp3} VHR group (n = 7/9 (78%), Figure S7).

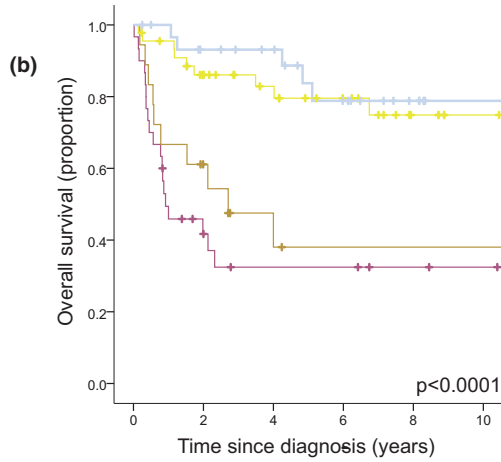
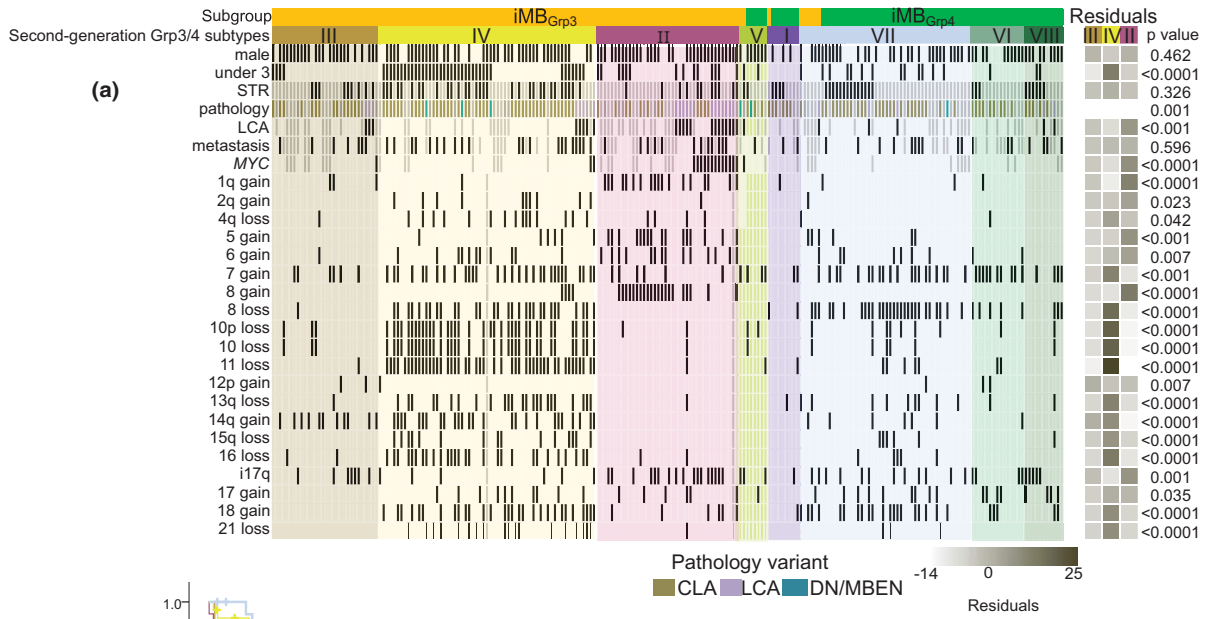
Given the low frequency of iMB_{Grp4}, intrasubgroup survival modelling was not possible. Taken together, iMB_{Grp4} patients belonged to a high-risk group with an OS of 70%, but there were distinct survival outcomes between Grp4-enriched subtypes (subtype VIII, 63% OS, high risk; subtypes VI and VII, OS 80%, standard risk). iMB_{Grp4} patients were typically older (median, 2.6 years) and almost all (19/20; 95%) were treated with upfront radiotherapy.

We next investigated all features as predictors of progression-free survival (PFS; i.e. relapse following upfront therapy) in iMB (Figure 4a-d). In univariable analysis of iMB_{Grp3}, a series of molecular (e.g. subtypes II, IV) and clinical (e.g. receipt of CSI radiotherapy (39/59, 66%) receipt of focal irradiation (15/59, 25%))

were significantly associated with PFS, with considerable overlap with findings observed for OS. In multivariable analyses, *MYC* amplification (HR 4.1, CI 1.4-11.6, $P = 0.008$) and chr11 loss (HR 0.1, CI 0.06-0.5, $P = 0.002$) (Figure 4a) were the only independent risk factors for PFS.

When PFS was considered in the entire iMB_{SHH} subgroup, STR (HR 7.2, CI 2.3-22.8, $P = 0.001$) and DN/MBEN pathology (HR 0.2, CI 0.08-0.61, $P = 0.004$) (Figure 4b) were the only independent risk factors, consistent with OS findings for iMB_{SHH}. When the DN/MBEN iMB_{SHH} patient group was discriminated and considered in isolation (n = 37), membership of iMB_{SHH-I} was significantly associated with a worse PFS (HR 3.6, CI 1.0-11.8, $P = 0.038$) (Figure 4c); the only significant predictor among all variables tested (Table S4). In contrast, the iMB_{SHH-I} subtype was not significant when considered across all iMB_{SHH} patients, supporting the importance of diagnosing the DN/MBEN variant within iMB_{SHH}.

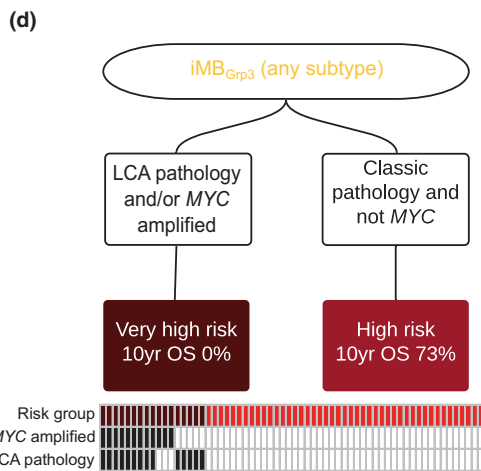
Sixty-two of iMB patients in our primary/discovery cohort relapsed or progressed (iMB_{SHH} n = 26; iMB_{Grp3} n = 25; iMB_{Grp4} n = 11; Figure 4e). The mean time from diagnosis to relapse was 1.5 years. Twenty-six per cent (14/54) of these patients received cranio-spinal radiotherapy at relapse; 5-year OS in this group was $24 \pm 5\%$ and 5-year post-relapse survival (PRS) was $17 \pm 4\%$. For iMB_{SHH}, DN/MBEN tumours had a greatly superior PRS (5-year PRS $60 \pm 14\%$ vs. $9 \pm 8\%$ for CLA/LCA) (Figure 4f, Figure S8). The iMB_{SHH} FR group (defined at diagnosis, Figure 2) had a significantly better PRS than VHR counterparts (Figure S8, 5yr PRS 60% vs. 5%, $P = 0.001$). Comparable findings were observed when patients who did not



No. at risk (censored)

Subtype II	30(0)	9(4)	6(5)	6(5)	4(7)	3(8)
Subtype III	18(0)	9(2)	4(4)	3(5)	3(5)	3(5)
Subtype IV	45(0)	32(7)	25(13)	19(18)	11(25)	7(29)
Subtype VII	31(0)	25(4)	22(7)	15(11)	9(17)	5(21)

Subtypes <5% frequency not shown



(c)

Overall survival in iMB_{Grp3}

Variable	n	Hazard Ratio	95% CI	p	adjusted p
Univariable analysis					
MYC amplification	12/62	16.5	6.6-41.2	<0.0001	<0.0001
LCA pathology	14/62	7.8	3.5-17.6	<0.0001	<0.0001
CTX and RTX	35/59	0.2	0.1-0.5	0.001	0.006
CSI RTX	38/59	0.3	0.1-0.6	0.001	0.006
iso17q	15/61	3.9	1.7-8.7	0.001	0.006
subtype II	14/55	4.7	1.9-11.1	0.001	0.006
CTX only	16/59	3.6	1.2-8.2	0.002	0.009
11q loss	29/61	0.3	0.1-0.6	0.003	0.009
11 loss	23/61	0.2	0.1-0.6	0.003	0.009
subtype IV	32/55	0.3	0.1-0.6	0.004	0.011
10 loss	20/61	0.2	0.1-0.7	0.014	0.039
WCA cytogenetic subgroup					
16q loss	23/61	0.4	0.2-1.1	0.065	0.152
13q loss	13/61	0.3	0.1-1.1	0.080	0.172
M+	24/58	2.0	0.9-4.5	0.09	0.180
Age under 3 years	26/62	1.9	0.8-4.3	0.139	0.278
Male	49/62	1.3	0.5-3.1	0.564	0.796
STR	46/59	1.3	0.5-3.4	0.634	0.937
subtype III	9/55	1.0	0.6-1.6	0.86	0.976
Multivariable analysis					
MYC amplification	9/55	4.9	2.0-12.0	<0.001	
LCA pathology	12/55	2.4	1.4-4.3	0.003	

Features entered into multivariable analysis (p < 0.1)

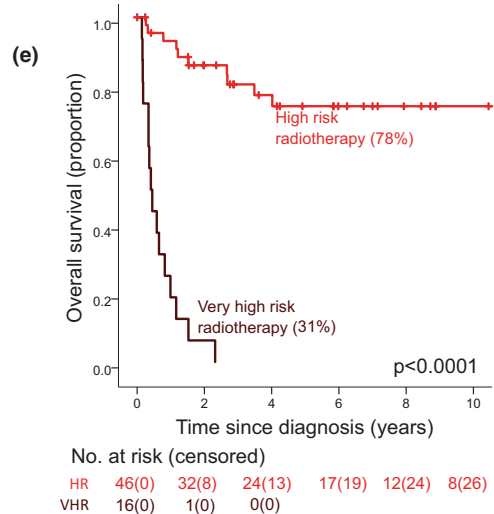


Figure 3. The molecular landscape of $iMB_{Group3/4}$ and associated retrospective clinical experience. (a) Clinico-pathological and molecular disease features are differently distributed in iMB_{Grp3} subtypes II, III and IV, as determined by use of the Grp3 and Grp4 classifier published by Sharma et al [10] in a combined cohort ($n = 146$) encompassing our primary discovery cohort and published cohorts from Northcott et al and Cavalli et al (Table S1). Residuals from Fisher's exact or χ^2 tests indicate where subgroup enrichment has occurred (darker shades indicate stronger relationships); scale bar for residuals is shown. Remaining second-generation molecular subtypes V, I and VII (rarely iMB_{Grp3}) and VI and VIII (exclusively iMB_{Grp4}) are shown for reference. Black bar, positive for feature; unfilled, negative for feature; grey bar, data unavailable (b) Kaplan-Meier plot of overall survival for second-generation molecular subtypes with frequency $>5\%$ from our primary discovery cohort and the Cavalli et al external discovery/validation cohort. Subtypes with a frequency of $>5\%$ of iMB are shown (II, III, IV and VII). At risk table (number censored in parentheses) and p value from log-rank test is shown. (c) Univariable and multivariable Cox proportional hazards regression model of overall survival in discovery cohort iMB_{Grp3} . Features which entered multivariable analysis ($P < 0.1$; $P < 0.05$ shown in bold font) are indicated. Cox proportional hazards test is shown either uncorrected (p) or corrected for multiple testing by the Benjamini-Hochberg method (adjusted p). Additional clinical features are shown for reference (gender, age under 3 years, metastasis). (d) Summary of a novel risk-stratification scheme for overall survival iMB_{Grp3} ($n = 62$). E. Kaplan-Meier plot of iMB_{Grp3} risk stratification. At risk table (number censored in parentheses) and log-rank test are shown. Abbreviations: STR, sub-total resection; CLA, classic; LCA, large cell/anaplastic; CI, confidence interval; HR, high risk; VHR, very high risk; RTX, radiotherapy; CTX, chemotherapy; M+, metastatic disease M2 or above

receive upfront radiotherapy were considered alone ($n = 24$, Figure 4g). Five-year PRS rates were equivalent between the novel iMB_{SHH} subtypes (iMB_{SHH-I} , $30\% \pm 16\%$ vs. iMB_{SHH-II} , $33\% \pm 15\%$, $P = 0.9$).

Post-relapse outcomes were dismal in iMB_{Grp3} (5yr PRS $10\% \pm 7\%$), irrespective of novel subtypes and treatment received at relapse; most deaths ($n = 14$, 82%) occurred within a year (median 2 months, IQR 0.5-7). Eighty-eight per cent ($n = 7/8$) of radio-naïve iMB_{Grp3} patients died within 3 months of relapse, despite a period of remission; only 2 patients received second-line radiotherapy due to rapid disease progression (Figure 4e). For iMB_{Grp4} , 11/29 patients relapsed (mean time to relapse, 2.5 years; all PRS < 2 years).

Integration of our validated subgroup-dependent OS and PFS prognostication schemes (Figure 2, iMB_{SHH} OS; Figure 3, iMB_{Grp3} and iMB_{Grp4} OS; PFS, Figure 4) allow the sub-classification of iMB patients into schema for the stratified delivery of risk-adapted therapies, based on the biomarkers discovered and therapies used in our retrospective cohorts (Figure 5a). Overall risk can be stratified straightforwardly using four validated features; consensus molecular subgroup, pathology variant, extent of resection and *MYC* amplification. This subgroup-directed model (Figure 5b) significantly outperformed the current, pathology-based, risk stratification [5] (5yr OS AUC 0.744 vs. 0.580) in our cohort, and was independently reproducible (FR 5yr OS 94%; HR 5yr OS 73%; VHR 5yr OS 46%; log-rank $P < 0.001$; Figure S6). Following definition of DN/MBEN iMB_{SHH} using this model, further distinction of the iMB_{SHH-I} and iMB_{SHH-II} subtypes enables prediction of PFS (Figure 4), while $MB_{Group3/4}$ subtypes associated

with 60-80% OS following upfront CSI are highlighted (Figure 3) for further clinical investigation (Figure 5a).

Discussion

Our analysis of almost 400 iMB tumours provides critical insights into their subgroup-dependent molecular heterogeneity, its clinical relevance and potential for exploitation towards disease sub-classification and improved, risk-adapted, therapies. Assessment of these large retrospective cohorts has enabled robust definition of the nature and reproducibility of molecular subtypes within iMB_{SHH} (types I, II) and iMB_{Group3} (types I-VII), and their interaction with established disease biomarkers. Consideration of their clinical associations across independent cohorts provides strong supporting evidence for their incorporation into future research studies and clinical application.

Radiation-sparing approaches have been postulated for iMB in an effort to obviate patients from deleterious, often life-limiting, late effects caused by treatment. Any biomarker discovery study based on retrospective cohorts must therefore consider the impact of radiation therapy. Our study identified risk-stratification groups that were reproducible and independent of receipt of radiotherapy. First, DN/MBEN was confirmed as a favourable-risk biomarker in our cohorts, highly associated with iMB_{SHH} . Importantly, a notable proportion of CLA and LCA iMB_{SHH} tumours were observed, which were associated with a very poor prognosis in both discovery and validation cohorts irrespective of therapy, clearly demonstrating that defining subgroup alone is insufficient for risk stratification in iMB_{SHH} . Central

(a) Progression-free survival in iMB_{Grp3}

Variable	Hazard Ratio	95% CI	p
Univariable analysis			
MYC amplification	11.4	4.9-26.7	1.9E-08
LCA pathology	5.5	2.5-11.8	1.8E-05
CTX only	3.7	1.3-2.8	0.001
11q loss	0.5	0.3-0.7	0.001
subtype IV	0.2	0.1-0.6	0.001
subtype II	3.7	0.6-8.3	0.002
CTX and RTX	0.6	0.3-0.8	0.002
focal RTX	0.2	0.1-0.5	0.002
11 loss	0.4	0.2-0.7	0.002
CSJ RTX	0.6	0.9-0.8	0.003
iso17q	3.1	1.3-6.7	0.005
17q gain	1.6	1.1-2.3	0.01
10 loss	0.6	0.3-0.9	0.028
13q loss	0.5	0.2-0.9	0.04
15q loss	0.5	0.2-1.0	0.075
Multivariable analysis			
Male	1.5	0.6-3.4	0.378
Age under 3	1.6	0.8-3.5	0.204
STR	1.4	0.5-3.3	0.386
Multivariable analysis			
MYC amplification	4.1	1.4-11.6	0.008
11 loss	0.1	0.6-0.5	0.002

Features entered into multivariate analysis (p<0.1)

(b) Progression-free survival in iMB_{SHH}

Variable	Hazard Ratio	95% CI	p
Univariable analysis			
DN/MBEN pathology	0.2	0.1-0.5	<0.001
STR	3.0	1.3-7.1	0.010
Gain 2	2.8	1.0-7.5	0.041
MBEN	0.4	0.1-1.2	0.094
iMB _{SHH-I}	2.4	0.9-6.0	0.067
M+	0.7	0.2-1.8	0.406
Age under 3	1.5	0.4-4.9	0.500
Male	0.9	0.4-1.8	0.853
Multivariable analysis			
STR	7.247	2.3-22.8	0.001
DN/MBEN pathology	0.218	0.1-0.6	0.004

Features entered into multivariate analysis (p<0.1)

(c) Progression-free survival in DN/MBEN iMB_{SHH}

Variable	Hazard Ratio	95% CI	p
Univariable analysis			
iMB _{SHH-I}	3.6	1.0-11.8	0.038
STR	2.4	0.6-8.9	0.190
Age under 3 years	26.8	0.0-19901.5	0.330
MBEN	0.5	0.1-1.9	0.331
Male	0.8	0.3-2.5	0.706
M+	0.9	0.3-3.0	0.900

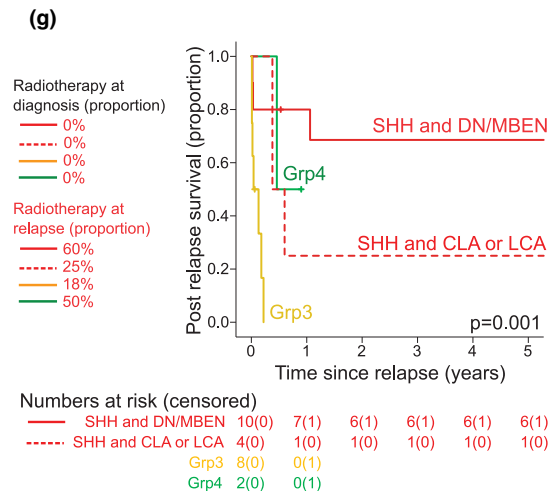
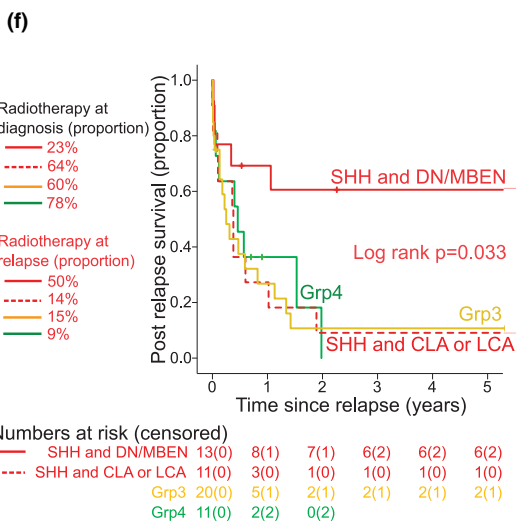
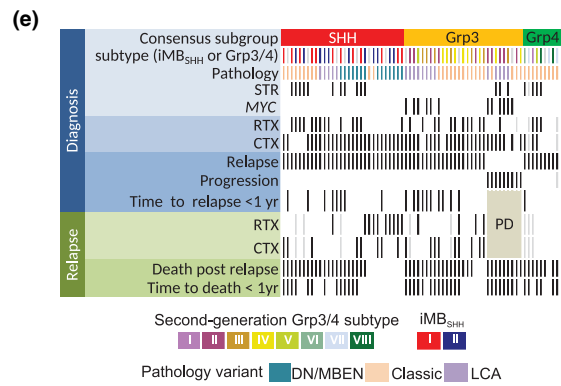
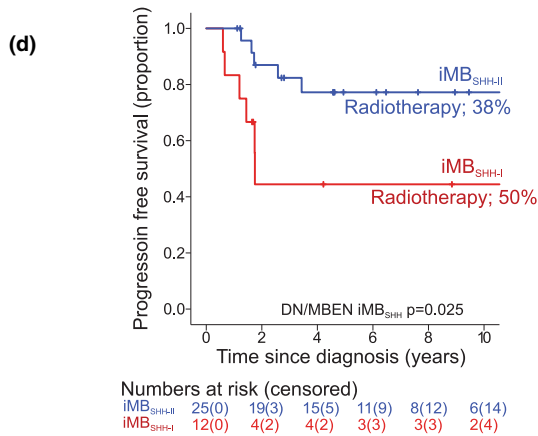


Figure 4. Progression-free survival and outcomes post-relapse, in iMB. **a, b.** PFS data from the discovery cohort was analysed. Univariable and multivariable Cox proportional hazards analysis of progression survival in iMB_{Grp3} (**a**), iMB_{SHH} (**b**) and in DN/MBEN iMB_{SHH} only (**c**). Features which entered multivariable analysis ($P < 0.1$; $P < 0.05$ shown in bold font) are indicated. (**d**) Progression-free survival Kaplan-Meier plot comparing iMB_{SHH-I} and iMB_{SHH-II} in a DN/MBEN only iMB_{SHH} cohort. (**e**) Summary of key clinical features in relapsed iMB ($n = 61$). Patients are shown in columns. Black bar, positive for feature; unfilled, negative for feature; grey bar, data unavailable. (**f**) Kaplan-Meier plot of post-relapse survival, comparing iMB_{SHH} split by pathology status, iMB_{Grp3} and, for reference, iMB_{Grp4}. (**g**) Kaplan-Meier plot of post-relapse survival in a radionave cohort (patients who did not receive radiotherapy at diagnosis, $n = 28$). For all Kaplan-Meier plots, at risk tables (number censored in parentheses), log-rank test and proportion receiving radiotherapy (focal or CSI and with or without adjunctive chemotherapy), at diagnosis, are shown. Abbreviations: STR, sub-total resection; CLA, classic; LCA, large cell/anaplastic; DN/MBEN, desmoplastic nodular/ medulloblastoma with extensive nodularity; SHH, sonic hedgehog; CI, confidence interval; RTX, radiotherapy; CTX, chemotherapy; M+, metastatic disease M2 or above; MYC, MYC amplification; PD, progressive disease

histological review to WHO 2016 [4] standards was essential for the robust definition of histological variants; in our experience, 8/62 iMB_{SHH} tumours were reclassified to DN/MBEN from their institutional CLA diagnosis.

Two discrete and reproducible molecular subtypes – iMB_{SHH-I} and iMB_{SHH-II} – were discriminated in our analysis of a unified iMB_{SHH} cohort totalling 155 tumours, encompassing patients from three independent studies [6,8]. This further supports the reproducibility of these molecular subtypes, as reported in previous studies [7,8,14,15], and defines their characteristics in large cohorts. Following discrimination of the favourable-risk iMB_{SHH} DN/MBEN group, definition of iMB_{SHH} molecular subtypes enabled prediction of PFS within our cohort, as a potential basis for the stratified delivery of upfront therapy. DN/MBEN iMB_{SHH-II} had significantly improved PFS over iMB_{SHH-I} independent of whether upfront radiotherapy was received. The prognostic significance of iMB_{SHH-I} and iMB_{SHH-II} subtypes differs between reported studies, which likely relates to differences in therapy and statistical power. Our study (large retrospective cohort; $n = 37$ DN/MBEN iMB_{SHH}, mixed therapies) and SJYC03 (clinical trial; $n = 42$ DN/MBEN iMB_{SHH}, risk-adapted therapies; no differences between low-, intermediate- and high-risk strata [7]) showed improved PFS for iMB_{SHH-II}. Conversely, HIT-2000 (clinical trial; $n = 28$ non-metastatic DN/MBEN iMB_{SHH}, intraventricular methotrexate therapy [15]) reported equivalent PFS for both groups. Two further cohorts, ACNS1221 (clinical trial, $n = 25$ DN/MBEN iMB_{SHH}, conventional systemic chemotherapy without intraventricular methotrexate [14]) and the HIT group/Burdenko Institute validation cohort (retrospective cohort, $n = 48$ DN/MBEN iMB_{SHH}, mixed therapies [15]) did not show a statistically significant

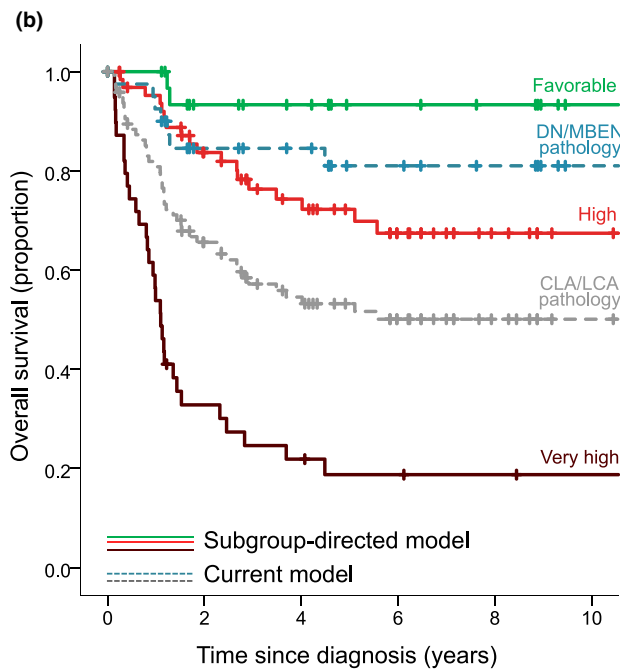
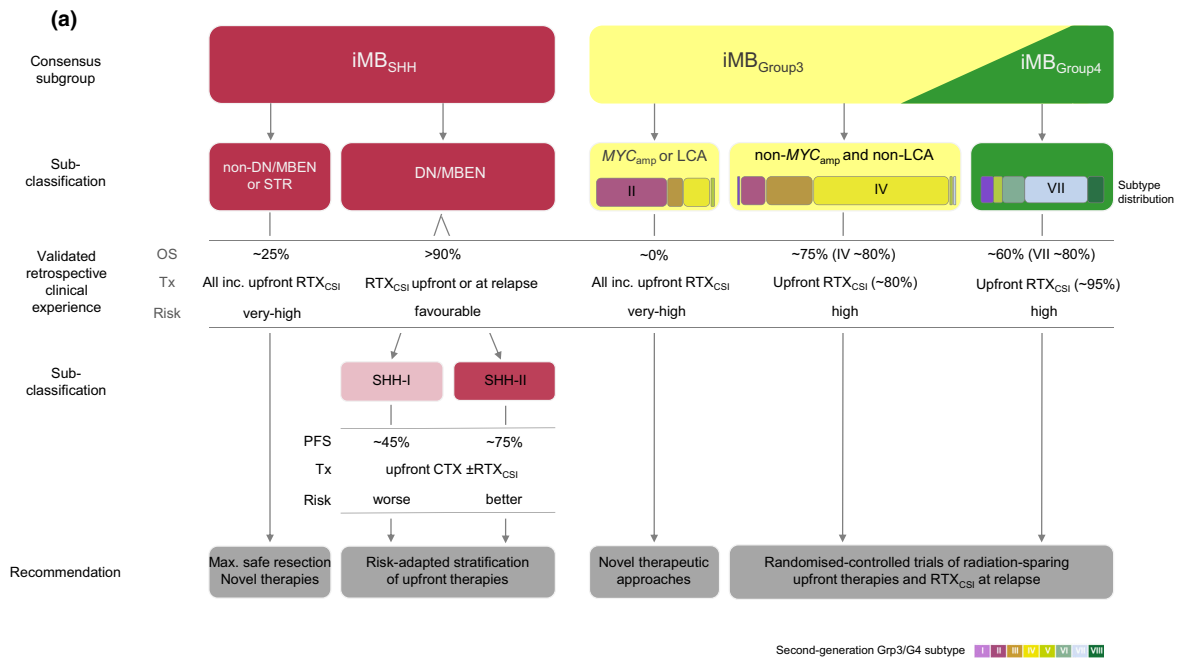
difference in PFS between iMB_{SHH-I} and iMB_{SHH-II} subtypes.

Controlled clinical trials using stratified therapeutic approaches should be considered for the DN/MBEN iMB_{SHH-II} patient group, aimed at resolving its interaction with different therapies and minimizing therapy-induced late effects, while maintaining OS rates. We observed equivalent rates of rescue, which commonly involved radiotherapy, in both iMB_{SHH} subtypes, further supporting such trials of risk-adapted therapies.

Our studies also reveal clinically actionable subgroups within iMB_{Grp3}. LCA pathology and MYC amplification are enriched in subtype II. Together or in isolation, they define a VHR group associated with a dismal prognosis (10yr OS 0%) and a short time to death, whether or not upfront radiation was received. These patients are refractory to current conventional treatments and often progress rapidly, with many not surviving to initiation of adjuvant therapy.

A series of better prognosis subgroups within iMB_{Grp3} and iMB_{Grp4} were noted. These include subtype IV (defined by many frequent CNAs [21]; 80% 5yr OS), subtype VII (iMB_{Grp4} enriched; 80% OS) and non-MYC/non-LCA iMB_{Grp3} (73% OS). However, the overwhelming majority (>75%) of these patients received standard upfront radiotherapy, and therefore the prognostic relevance of these groups in the radionave iMB setting, and the associated use of post-relapse radiotherapy as a rescue strategy, requires further assessment.

We also assessed iMB prognostic factors defined in previous historical studies, in our cohort [5]. Metastatic disease was enriched in iMB_{Grp3}, but was not significantly associated with poorer survival (Figure 3). Its prognostic relevance, and its interaction with radiotherapy, thus remains unconfirmed in this patient group. Similarly, in a previous iMB cohort, STR was



Numbers at risk (censored)

	0	2	4	6	8	10
Favorable	34(0)	25(7)	22(10)	17(15)	15(17)	10(22)
High	66(0)	47(9)	36(15)	24(24)	14(34)	9(39)
Very high	39(0)	12(1)	8(1)	6(2)	5(3)	4(4)
DN/MBEN	42(0)	28(8)	25(11)	19(16)	16(19)	11(24)
CLA/LCA	98(0)	56(9)	41(15)	28(25)	18(35)	12(41)

Figure 5. Subgroup-dependent prognostic models for iMB and candidate groups for risk-adapted therapies. (a) A novel subgroup-directed risk-stratification scheme for iMB, incorporating validated OS and PFS correlates identified in our cohorts. (b) Patients mapped to the OS scheme using four routinely testable features; molecular subgroup, pathology variant, resection status and *MYC* amplification status. A Kaplan-Meier plot showing our entire iMB cohort stratified for OS using this subgroup-directed model and the current, pathology-based model, alongside an at-risk table (number censored in parentheses). Abbreviations used: DN/MBEN, desmoplastic/nodular, medulloblastoma with extensive nodularity; LCA, large-cell/anaplastic; CLA, classic; STR, sub-total resection; GTR, gross total resection; *MYC*, *MYC* amplification; OS, overall survival; PFS, progression-free survival; Tx, treatment; RTX, radiotherapy; CTX, chemotherapy; RTX_{CSI}, cranio-spinal radiotherapy

significantly associated with poorer OS [5]. Our analysis demonstrated its independent prognostic significance in iMB_{SHH}; while this may reflect historic surgical practices, outcomes for, and rates of, STR were equivalent across our collection period. Receipt of upfront focal radiotherapy was not associated with improved PFS within iMB_{SHH} (data not shown). However, receipt of focal radiotherapy was associated with improved PFS (compared to no irradiation) in iMB_{Grp3} in univariable analyses. This finding is likely contributed to by the high frequency of very-high-risk iMB_{Grp3} patients in our cohort who received no radiotherapy at all, likely due to a clinical decision to palliate at diagnosis.

To allow maximal inclusion and assessment of clinico-biological relationships we selected patients up to 5 years of age for analysis, however, applying our subgroup-directed survival model reached equivalent findings when restricted to patients under 3 years old in our cohort (Figure S9). This, coupled with the recent identification of age-dependent molecular subtypes within MB_{SHH} (MB_{SHH-Infant}, <4.3 years vs. MB_{SHH-Childhood}) [9], suggests that the definition of the infant disease should include patients at the upper end of the 3–5 age range in current clinical use.

As discussed for DN/MBEN iMB_{SHH} and its subtypes, both treatment and prognostic effects may differ between clinical studies. Similarly, our retrospective study encompassed patient cohorts treated with mixed protocols. As far as possible, we controlled for age and therapy type in our survival analyses and risk modelling, and validated findings across large independent cohorts. This has enabled the identification and validation of clinically actionable biological subgroups with distinct and reproducible disease behaviours (favourable-risk DN/MBEN iMB_{SHH}, very-high-risk LCA/*MYC* iMB_{Grp3}), which are independent of treatment. Cohort-specific or treatment-dependent effects, particularly with regard to emerging therapeutic concepts in iMB (e.g. high-dose chemotherapy, intrathecal therapies)

must be considered in future clinically controlled studies.

In summary, assessment of the molecular pathology of iMB in large historic cohorts has allowed the robust characterization of each iMB molecular subgroup and the novel molecular subtypes they harbour. Almost a third of iMB can be reclassified into a VHR group, which, based on their dismal outcomes and rapid disease course, should be urgently considered for novel upfront therapeutic approaches, such as anti-*MYC* therapeutics [22]. Prognostic subtypes within FR groups (e.g. DN/MBEN iMB_{SHH-I}, iMB_{SHH-II}) offer opportunities to direct the stratified use of upfront therapies. Identified HR iMB groups, with 60–80% survival rates using CSI-based regimes, are suitable for investigation in randomized clinical trials.

Consent for publication

NA.

Acknowledgements

The authors would like to thank all of the patients and families who contributed to this study.

Conflict of interests

All other authors declare that they have no competing interests.

Funding

This study was funded by Cancer Research UK C8464/A13457 C8464/A23391, The Tom Grahame Trust, JGW Patterson Foundation, Action Medical Research and the INSTINCT network (funded by The Brain Tumour Charity, Children with Cancer UK and Great Ormond Street Hospital Children's Charity).

Authors' contributions

Conception and design: DH, ECS, DW, SB and SCC. Collection and assembly of data: DH, JL, CIH, RMH, AS, PA, SR, MD, CS, SC and SB. Data analysis and interpretation: DH, GR, ECS, LP, DW, SB and SCC. Central pathological review: AJ, SW and TJ. Provision of study materials or patients: BP, AM and SB. Manuscript writing: All authors. Final approval of manuscript: All authors. Accountable for all aspects of the work: All authors.

Ethics approval and consent to participate

Human tumour samples were provided by the UK CCLG as part of CCLG-approved biological study BS-2007-04; informed consent was obtained from all subjects and investigations conducted with approval from Newcastle/North Tyneside Research Ethics Committee (study reference 07/Q0905/71).

Data Availability Statement

The data that support the findings of this study are available from the corresponding author upon reasonable request.

References

- Pizer BL, Clifford SC. The potential impact of tumour biology on improved clinical practice for medulloblastoma: progress towards biologically driven clinical trials. *Br J Neurosurg* 2009; **23**: 364–75
- Jenkin D, Danjoux C, Greenberg M. Subsequent quality of life for children irradiated for a brain tumor before age four years. *Med Pediatr Oncol* 1998; **31**: 506–11
- Mulhern RK, Horowitz ME, Kovnar EH, Langston J, Sanford RA, Kun LE. Neurodevelopmental status of infants and young children treated for brain tumors with preirradiation chemotherapy. *J Clin Oncol* 1989; **7**: 1660–6
- Louis DN, Perry A, Reifenberger G, von Deimling A, Figarella-Branger D, Cavenee WK, et al. The 2016 World Health Organization Classification of Tumors of the Central Nervous System: a summary. *Acta Neuropathol* 2016; **131**: 803–20
- Rutkowski S, von Hoff K, Emser A, Zwiener I, Pietsch T, Figarella-Branger D, et al. Survival and prognostic factors of early childhood medulloblastoma: an international meta-analysis. *J Clin Oncol* 2010; **28**: 4961–8
- Northcott PA, Buchhalter I, Morrissy AS, Hovestadt V, Weischenfeldt J, Ehrenberger T, et al. The whole-genome landscape of medulloblastoma subtypes. *Nature* 2017; **547**: 311–7
- Robinson GW, Rudneva VA, Buchhalter I, Billups CA, Waszak SM, Smith KS, et al. Risk-adapted therapy for young children with medulloblastoma (SJYC07): therapeutic and molecular outcomes from a multicentre, phase 2 trial. *Lancet Oncol* 2018; **19**: 768–84
- Cavalli FMG, Remke M, Rampasek L, Peacock J, Shih DJH, Luu B, et al. Intertumoral Heterogeneity within Medulloblastoma Subgroups. *Cancer Cell* 2017; **31**: 737–54.e6
- Schwalbe EC, Lindsey JC, Nakjang S, Crosier S, Smith AJ, Hicks D, et al. Novel molecular subgroups for clinical classification and outcome prediction in childhood medulloblastoma: a cohort study. *Lancet Oncol* 2017; **18**: 958–71
- Sharma T, Schwalbe EC, Williamson D, Sill M, Hovestadt V, Mynarek M, et al. Second-generation molecular subgrouping of medulloblastoma: an international meta-analysis of Group 3 and Group 4 subtypes. *Acta Neuropathol* 2019; **138**: 309–26
- Clifford SC, Lannering B, Schwalbe EC, Hicks D, O'Toole K, Nicholson SL, et al. Biomarker-driven stratification of disease-risk in non-metastatic medulloblastoma: Results from the multi-center HIT-SIOP-PNET4 clinical trial. *Oncotarget* 2015; **6**: 38827–39
- Ellison DW, Kocak M, Dalton J, Megahed H, Lusher ME, Ryan SL, et al. Definition of Disease-Risk Stratification Groups in Childhood Medulloblastoma Using Combined Clinical, Pathologic, and Molecular Variables. *J Clin Oncol* 2011; **29**: 1400–7
- Robinson GW, Orr BA, Wu G, Gururangan S, Lin T, Qaddoumi I, et al. Vismodegib Exerts Targeted Efficacy Against Recurrent Sonic Hedgehog-Subgroup Medulloblastoma: Results From Phase II Pediatric Brain Tumor Consortium Studies PBTC-025B and PBTC-032. *J Clin Oncol* 2015; **33**: 2646–54
- Lafay-Cousin L, Bouffet E, Strother D, Rudneva V, Hawkins C, Eberhart C, et al. Phase II Study of Non-metastatic Desmoplastic Medulloblastoma in Children Younger Than 4 Years of Age: A Report of the Children's Oncology Group (ACNS1221). *J Clin Oncol* 2020; **38**: 223–31
- Mynarek M, von Hoff K, Pietsch T, Ottensmeier H, Warmuth-Metz M, Bison B, et al. Nonmetastatic Medulloblastoma of Early Childhood: Results From the Prospective Clinical Trial HIT-2000 and An Extended Validation Cohort. *J Clin Oncol* 2020; **38**: 2028–40
- Dhall G, O'Neil SH, Ji L, Haley K, Whitaker AM, Nelson MD, et al. Excellent Outcome of Young Children with Nodular Desmoplastic Medulloblastoma Treated on "Head Start" III: A Multi-Institutional. *Prospective Clinical Trial Neuro Oncol* 2020. <https://doi.org/10.1093/neuonc/noaa102>

- 17 Schwalbe EC, Williamson D, Lindsey JC, Hamilton D, Ryan SL, Megahed H, et al. DNA methylation profiling of medulloblastoma allows robust subclassification and improved outcome prediction using formalin-fixed biopsies. *Acta Neuropathol* 2013; **125**: 359–71
- 18 Hovestadt V, Remke M, Kool M, Pietsch T, Northcott PA, Fischer R, et al. Robust molecular subgrouping and copy-number profiling of medulloblastoma from small amounts of archival tumour material using high-density DNA methylation arrays. *Acta Neuropathol* 2013; **125**: 913–6
- 19 Lamont JM, McManamy CS, Pearson AD, Clifford SC, Ellison DW. Combined histopathological and molecular cytogenetic stratification of medulloblastoma patients. *Clin Cancer Res*. 2004; **10**: 5482–93
- 20 Langdon JA, Lamont JM, Scott DK, Dyer S, Prebble E, Bown N, et al. Combined genome-wide allelotyping and copy number analysis identify frequent genetic losses without copy number reduction in medulloblastoma. *Genes Chromosomes Cancer* 2006; **45**: 47–60
- 21 Goschzik T, Schwalbe EC, Hicks D, Smith A, Zur Muehlen A, Figarella-Branger D, et al. Prognostic effect of whole chromosomal aberration signatures in standard-risk, non-WNT/non-SHH medulloblastoma: a retrospective, molecular analysis of the HIT-SIOP PNET 4 trial. *Lancet Oncol* 2018; **19**: 1602–16
- 22 Barone G, Anderson J, Pearson AD, Petrie K, Chesler L. New strategies in neuroblastoma: Therapeutic targeting of MYCN and ALK. *Clin Cancer Res* 2013; **19**: 5814–21

Supporting information

Additional Supporting Information may be found in the online version of this article at the publisher's web-site:

Supplementary Material. Detailed methods and supplementary tables and figures are available in the supporting information.

Received 5 May 2020

Accepted after revision 29 July 2020

Published online Article Accepted on 11 August 2020